View metadata, citation and similar papers at core.ac.uk
brought to you by CORE
provided by ELTE Digital Institutional Repository (EDIT)

*Proc. Budapest'02 Workshop on Quark & Hadron Dynamics* (2002) 000–000

**Budapest'02 Workshop on Quark & Hadron Dynamics**
**Budapest, Hungary**
**March 3–7, 2002**

arXiv:nucl-th/0206006v1 4 Jun 2002

# Perturbative QCD Results on Pion Production in $pp$, $pA$ and $AA$ Collisions

G.G. Barnaföldi[1,2], P. Lévai[1], G. Papp[3], G. Fai[4] and Y. Zhang[4]

[1] KFKI Research Institute for Particle and Nuclear Physics, P.O. Box 49, Budapest, 1525, Hungary
[2] Laboratory for Information Technology, Eötvös University, Pázmány Péter sétány 1/A, Budapest, 1117 Hungary
[3] HAS Research Group for Theoretical Physics, Eötvös University Pázmány Péter sétány 1/A, Budapest, 1117 Hungary
[4] Center for Nuclear Research, Department of Physics, Kent State University, Kent, OH 44242, USA

**Abstract.** We summarize new pQCD results on pion production in proton-proton ($pp$), proton-nucleus ($pA$) and nucleus-nucleus ($AA$) collisions. Our calculation introduces intrinsic parton transverse momentum ($k_T$) and is performed effectively at next-to-leading order (NLO), applying a $K$ factor extracted for jet events. Two different factorization scales, $Q = p_{T,jet}/2$ and $p_{T,jet}$ are used. Experimental data in $pA$ collisions imply a preference for the latter choice at NLO level. We display our results at CERN SPS for $AA$ collisions.

*Keywords:* pQCD, intrinsic $k_T$, pion production, $K$ factor, Cronin effect
*PACS:* 24.85.+p, 13.85.Ni, 13.85.Qk, 25.75.Dw

## 1. Introduction

Recent RHIC and CERN experiments require solid theoretical baseline calculations, able to reproduce proton-proton, proton-nucleus and the measured nucleus-nucleus data accurately enough to find possible deviations due to new collective phenomena or to a new state of the matter. In this paper pion production is calculated in a pQCD-improved parton model [ 1]. Recently we have performed a leading order (LO) calculation and displayed the results of a systematic analysis of $pp$ ($p\overline{p}$), $pA$ and $AA$ data on pion production [ 2]. The key points were the introduction of the intrinsic transverse momentum distribution of the partons and the folding of nuclear

multiscattering effects into the pQCD calculations. We have also calculated pion production in next-to-leading order (NLO) [ 3]. However, the NLO cross sections were estimated by applying an oversimplified constant $K$ factor ($K = 2$) to the LO cross sections. Since the determination of nuclear effects (e.g. the strength of nuclear multiscattering) and other collective effects require great precision (better than $10 - 20$ %), we need to repeat the earlier calculation using appropriate NLO cross sections. In Section 2 we summarize our results on energy and momentum dependent $K$ factors.

In standard calculations for $pp$ collisions the factorization scale is typically chosen in the range $p_T/3 \leq Q \leq 2p_T$. We find that at the NLO level the reproduction of nuclear effects in $pA$ collisions (specifically the Cronin effect [ 4, 5]) strongly depends on the choice of the factorization scale. We discuss this issue in Section 3.

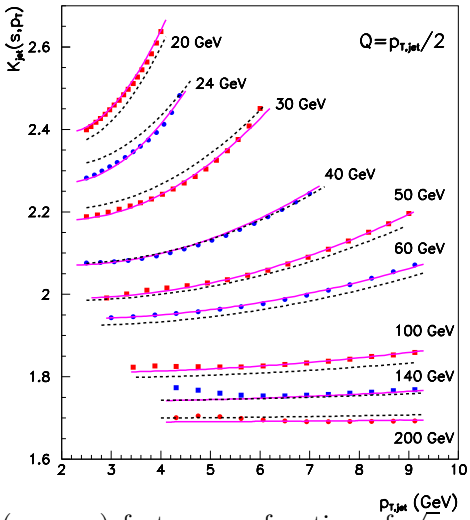


**Fig. 1.** The $K_{jet}(s, p_{T,jet})$ factor as a function of $\sqrt{s}$ and $p_{T,jet}$ at scale $Q = p_{T,jet}/2$. Solid lines guide the eye through the calculated points and the fitted parabolae of eq. (2) are indicated by dashed lines [ 6].

## 2. $K$ factor for NLO jet-production in $pp$ collision

In a previous paper [ 6] we have extracted a $K$ factor for jet production in $pp$ collisions. The scale in the parton distribution functions (PDFs) was chosen to be $Q = p_{T,jet}/2$ for jets with jet-cone angle $R = 1$ and separation $R_{sep} = 2R$. An energy and transverse momentum dependent correction factor, $K_{jet}(s, p_{T,jet})$, was then obtained as

$$\frac{\mathrm{d}\sigma^{NLO}}{\mathrm{d}\hat{t}} = K_{jet}\left(s, p_{T,jet}\right) \frac{\mathrm{d}\sigma^{Born}}{\mathrm{d}\hat{t}} , \qquad (1)$$

where the cross sections are understood at the jet level (see eq. (4)).

Full NLO calculations were performed by the Ellis – Kunszt – Soper (EKS) [ 7, 8] and the Aversa – Chiappetta – Greco – Guillet (ACGG) [ 9] groups, and are based on the matrix elements published in Ref. [ 10]. We used a public Fortran code from the EKS group [ 11] with MRST (central gluon) PDFs [ 12] to calculate the Born and the NLO contributions. The extracted $K$ factor of eq. (1) is shown in Fig. 1 in the energy range 20 GeV $\leq \sqrt{s} \leq$ 200 GeV.

For practical purposes, the $K$ factors were parameterized (within 2-4 % precision) as

$$K_{jet}(s, p_{T,jet}) = 1.6 + \frac{20.}{\sqrt{s}} - \frac{24.}{(\sqrt{s} - 10.)^2}\, p_{T,jet} + \frac{6.}{(\sqrt{s} - 10.)^2}\, p_{T,jet}^2 \ , \qquad (2)$$

where $p_{T,jet}$ and $\sqrt{s}$ are in GeV and the constants are understood with their appropriate units.

In this paper we plan to use a different scale in the PDFs (see Section 3), namely $Q = p_{T,jet}$. Thus we repeat our calculation of the jet-level $K$ factor at this new scale, using $R = 1$. The results are displayed in Fig. 2.

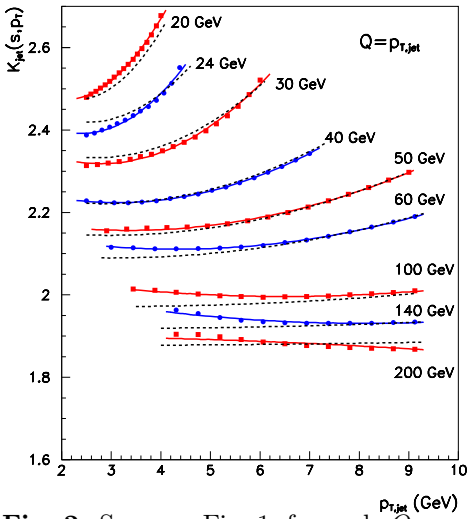


**Fig. 2.** Same as Fig. 1, for scale $Q = p_{T,jet}$.

These new results may be again parameterized quadratically with good precision:

$$K_{jet}(s, p_{T,jet}) = 1.79 + \frac{20.}{\sqrt{s}} - \frac{45.}{(\sqrt{s} - 7.)^2}\, p_{T,jet} + \frac{7.}{(\sqrt{s} - 9.)^2}\, p_{T,jet}^2 \ . \qquad (3)$$

Figures 1 and 2 demonstrate that increasing the scale by a factor of 2, the jet-level $K$ factor is increased by $\sim$ $10 - 15$ %, maintaining the characteristic dependence on $s$ and $p_T$. At RHIC energies ($\sqrt{s} = 200$ AGeV) the $K$ factor is almost constant with values $\sim 1.7$ (at $Q = p_{T,jet}/2$) and $\sim 1.9$ (at $Q = p_{T,jet}$).

## 3. Pion production from CERN to Tevatron energies

Here, we summarize the method used to calculate pion production in a pQCD-improved parton model, following our previous work in LO, see Ref. [ 2]. In Subsection 3.1 we introduce the intrinsic transverse momentum distribution for partons and fit the width of the applied Gaussian distribution to available $pp$ (or $p\bar{p}$) data in the c.m. energy range 20 GeV $\leq \sqrt{s} \leq$ 1.8 TeV. A large collection of pion and charged hadron production data can be utilized in this energy range to extract information about the intrinsic transverse momentum distribution, e.g the energy dependence of the Gaussian width. In Subsection 3.2 the Cronin effect [ 4, 5] is discussed in $pA$ collisions. Subsection 3.3 deals with hard pion production in $AA$ collisions at CERN SPS energies.

### *3.1. Parton model calculations with intrinsic transverse momentum*

In $pp$ collision we describe the invariant cross section for pion production in a pQCD-improved parton model on the basis of the factorization theorem [ 1]:

$$E_\pi \frac{\mathrm{d}\sigma_\pi^{pp}}{\mathrm{d}^3 p} = \sum_{abcd} \int \mathrm{d}x_a \, \mathrm{d}x_b \, \mathrm{d}z_c \; f_{a/p}(x_a, Q^2) \; f_{b/p}(x_b, Q^2) \; \times$$
$$\times \quad \left[ K_{jet}(s, p_{T,jet}) \; \frac{\mathrm{d}\sigma}{\mathrm{d}\hat{t}}^{ab\to cd} \right] \frac{D_{\pi/c}(z_c, Q'^2)}{\pi z_c^2} \; \hat{s} \; \delta(\hat{s} + \hat{t} + \hat{u}) \; . \quad (4)$$

Here $f_{a/p}(x_a, Q^2)$ and $f_{b/p}(x_b, Q^2)$ are the LO/NLO parton distribution functions for the colliding partons $a$ and $b$ within the interacting protons as functions of momentum fraction $x$, at scale $Q$. $\mathrm{d}\sigma/\mathrm{d}\hat{t}$ is the hard scattering cross section of the partonic subprocess $ab \to cd$ in LO (Born term) and the $K_{jet}$ factor is applied to include NLO contributions. In eq. (4) we use the convention that the parton-level Mandelstam variables are indicated by a 'hat' (like $\hat{t}$ above). The LO/NLO fragmentation function (FF), $D_{\pi/c}(z_c, Q'^2)$ gives the probability for parton $c$ to fragment into $\pi$ with momentum fraction $z_c$ and fragmentation scale $Q'$. For the results presented here we fix $Q' = p_T/2$ and use the KKP parametrization [ 13].

For LO calculations, $K_{jet}(s, p_{T,jet}) \equiv 1$. As discussed in Section 2, in NLO calculations the Born partonic cross section is multiplied by $K_{jet}(s, p_{T,jet})$ inside the integral of eq. (4). For LO calculation the GRV [ 14], for NLO the MRST [ 12] PDF sets were applied at scales $Q = p_{T,jet}/2$ and $Q = p_{T,jet}$, respectively, where $p_{T,jet} = p_T/z_c$.

In a phenomenological approach, eq. (4) can be generalized to incorporate intrinsic transverse momentum by using a product assumption and extending each integral over the parton distribution functions to $k_T$-space [ 15, 16],

$$\mathrm{d}x \; f_{a/p}(x, Q^2) \to \mathrm{d}x \; \mathrm{d}^2 k_T \; g(\vec{k}_T) \; f_{a/p}(x, Q^2) \; , \quad (5)$$

where $g(\vec{k}_T)$ is the intrinsic transverse momentum distribution of the relevant parton in the proton. We follow this approach in the present work, choosing $g(\vec{k}_T)$ to be a

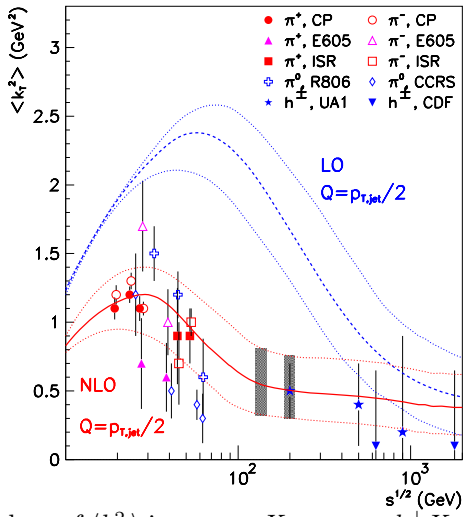


**Fig. 3.** Best fit values of $\langle k_T^2 \rangle$ in $pp \to \pi X$ or $p\bar{p} \to h^{\pm} X$ reactions at LO ( dashed line) and NLO (solid line) levels with factorization scale $Q = p_{T,jet}/2$, both with errors (dotted lines). Due to the overlap at the same energy, some points with error bars have been slightly shifted for better visibility. Thin lines represent the error estimate of the curves, while the thick bars are for RHIC energies in NLO.

Gaussian:

$$g(\vec{k}_T) = \frac{1}{\pi \langle k_T^2 \rangle} e^{-k_T^2/\langle k_T^2 \rangle} \quad , \tag{6}$$

with $\langle k_T^2 \rangle$ being the 2-dimensional width of the $k_T$ distribution. Increasing the value of parameter $\langle k_T^2 \rangle$, the particle production also increases in the transverse momentum window 2 GeV $\leq p_T \leq$ 6 GeV.

In Figs. 3 and 4, we present the best fit values of $\langle k_T^2 \rangle$, calculated in pion and charged hadron ($h^{\pm}$) production in $pp$ and $p\bar{p}$ collisions at scales $Q = p_{T,jet}/2$ and $Q = p_{T,jet}$, respectively, using several independent experimental data [ 5, 17, 18, 19, 20, 21, 22, 23, 24, 25]. As expected, the obtained value of $\langle k_T^2 \rangle$ at NLO level is less than at LO level if $Q = p_{T,jet}/2$ is used in both calculations (see Fig. 3). However, this difference in $\langle k_T^2 \rangle$ almost disappears changing the NLO scale to $Q = p_{T,jet}$, but keeping the LO scale at $Q = p_{T,jet}/2$ (see Fig. 4).

As an example to illustrate the degree of accuracy of the description in the $pp$ sector, Fig. 5 compares calculated $\pi^+$ and $\pi^-$ spectra and $\pi^-/\pi^+$ ratios to the data [ 5] at the c.m. energy $\sqrt{s} = 27.4$ GeV, respectively, obtained with the values of $\langle k_T^2 \rangle$ (the different scales are indicated in the top panel). We find that the data/theory and $\pi^-/\pi^+$ ratios are well reproduced for 2 GeV $\leq p_T \leq$ 6 GeV. Based on this and similar examples, we believe that hard pion production in $pp$ collisions is reasonably under control at the present level of calculation.

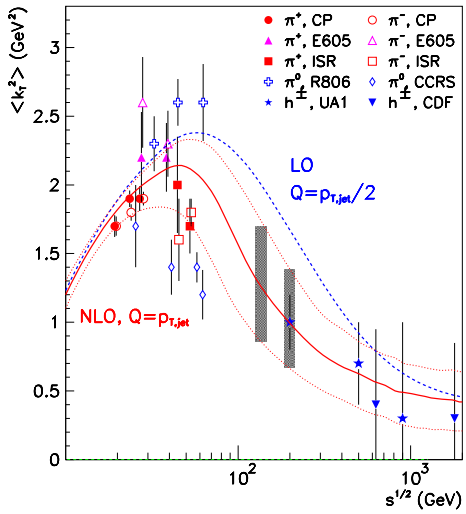


**Fig. 4.** Same as Fig. 3 for scale $Q = p_{T,jet}$ at NLO level compared to the LO results at $Q = p_{T,jet}/2$ from Fig. 3.

### *3.2. Hard pions from pA collisions – Cronin effect*

Interest in the nuclear dependence of hard particle production was motivated by the discovery of the Cronin effect [ 4, 5]: it was found experimentally that in the transverse momentum window 2 GeV $\leq p_T \leq$ 6 GeV more particles are produced than it was expected from a simple scaling of the $pp$ data. As discussed in the introduction, reproducing the Cronin effect could be the key point – at least in the sense of scale fixing – in our calculations.

In our model there is an extra contribution to the basic Gaussian width of the intrinsic parton transverse momentum distribution due to the nuclear environment. This extra width can be related to the number of nucleon-nucleon (NN) collisions in the medium. To characterize the $\langle k_T^2 \rangle$ enhancement, we write the modified width of the parton transverse momentum distribution of the incoming proton as

$$\langle k_T^2 \rangle_{pA} = \langle k_T^2 \rangle_{pp} + C \cdot h_{pA}(b) \ . \tag{7}$$

Here $\langle k_T^2 \rangle_{pp}$ is the width of the transverse momentum distribution of partons in $pp$ collisions from Subsection 3.1 (also denoted simply by $\langle k_T^2 \rangle$), $h_{pA}(b)$ describes the number of effective NN collision at impact parameter $b$, each of which imparts an average increase in the transverse momentum width denoted by $C$. In $pA$ reactions, one parton from the projectile proton and another one from the target nucleus participate in the hard collision. We apply $\langle k_T^2 \rangle_{pA}$ for the projectile parton, which incorporates the additional NN collisions indicated in eq. (7). For the target parton the original $\langle k_T^2 \rangle_{pp}$ is used from Fig. 3 or Fig. 4.

The effectivity function $h_{pA}(b)$ can be written in terms of the number of collisions suffered by the incoming proton in the target nucleus, $\nu_A(b) = \sigma_{NN} t_A(b)$,

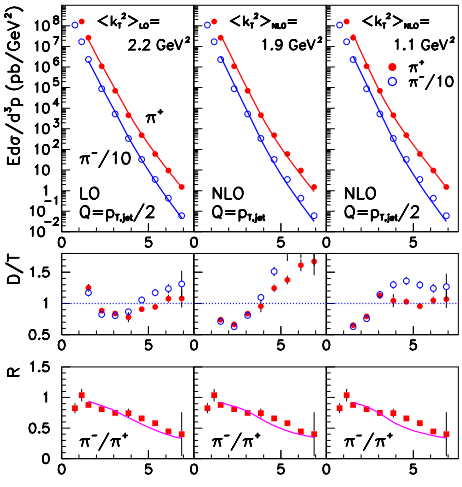


**Fig. 5.** LO and NLO calculations at different scales (see text). Top panel: invariant cross section of $\pi^+$ and $\pi^-$ production from $pp$ collisions (Negative pion data are divided by 10 for better visibility). Central panel: data/theory ratios, $D/T$. Lower panel: $\pi^-/\pi^+$ ratios as functions of transverse momentum at c.m. energies $\sqrt{s}$ =27.4 GeV. Data are from [ 5].

where $\sigma_{NN}$ is the inelastic nucleon-nucleon cross section:

$$h_{pA}(b) = \begin{cases} \nu_A(b) - 1 & \nu_A(b) < \nu_{max} \\ \nu_{max} - 1 & \text{otherwise} \end{cases} \quad . \tag{8}$$

The value $\nu_{max} = \infty$ corresponds to the case where all possible semihard collisions contribute to the broadening. Requiring independence of target we found that for realistic nuclei the maximum number of semihard collisions is $2 \leq \nu_{max} \leq 5$.

According to the Glauber picture, the hard pion production cross section from $pA$ reactions can be written as an integral over impact parameter $b$:

$$E_\pi \frac{\mathrm{d}\sigma_\pi^{pA}}{\mathrm{d}^3 p} = \int \mathrm{d}^2 b \; t_A(b) \; E_\pi \frac{\mathrm{d}\sigma_\pi^{pp}(\langle k_T^2 \rangle_{pA}, \langle k_T^2 \rangle_{pp})}{\mathrm{d}^3 p} \quad , \tag{9}$$

where the proton-proton cross section on the right hand side represents the cross section from eq. (4) with the transverse momentum extension as given by eq.-s (5) and (6). Here $t_A(b) = \int \mathrm{d}z \, \rho(b,z)$ is the nuclear thickness function (in terms of the density distribution $\rho$) normalized as $\int \mathrm{d}^2 b \, t_A(b) = A$. Furthermore, the PDFs are modified in the nuclear environment ("shadowing") [ 27, 28]. This effect and isospin asymmetry are taken into account on average using a scale independent parameterization of the shadowing function $S_{a/A}(x)$ adopted from Ref. [ 27]:

$$f_{a/A}(x,Q^2) = S_{a/A}(x) \left[ \frac{Z}{A} f_{a/p}(x,Q^2) + \left(1 - \frac{Z}{A}\right) f_{a/n}(x,Q^2) \right] \quad , \tag{10}$$

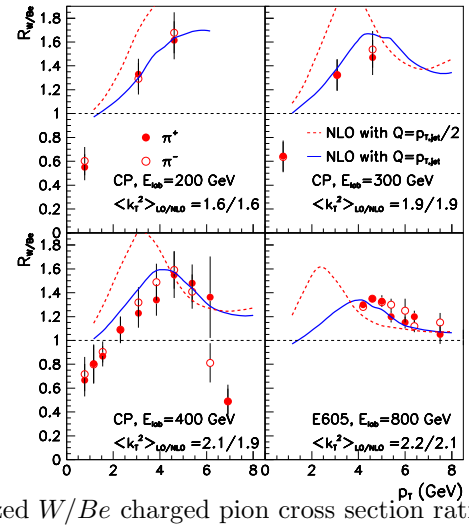


**Fig. 6.** Normalized $W/Be$ charged pion cross section ratios at different energies: $\sqrt{s} = 19.4; 23.8; 27.4;$ and 38.8 GeV [ 5, 19, 20, 26]. The calculations are at NLO level with scale $Q = p_{T,jet}/2$ (dashed lines) and with $Q = p_{T,jet}$ (solid line). The deviation from unity represents the Cronin enhancement.

where $f_{a/n}(x, Q^2)$ is the PDF for the neutron and Z is the number of protons.

The Cronin enhancement is presented in Fig. 6 by the normalized (with mass number $A$) $W/Be$ charged pion cross section ratios together with the data at several energies for $\pi^+$ (dots) and $\pi^-$ (open circles) [ 5, 19, 20, 26]. In our NLO calculations we used the previously fixed $\langle k_T^2 \rangle$ values at scales $Q = p_{T,jet}/2$ (dashed lines) and $Q = p_{T,jet}$ (solid lines). Here the Cronin parameter is $C = 0.35$ GeV$^2$ and $\nu_{max} = 3$.

In the absence of the Cronin effect, these ratios would be identically 1. The significant deviation of the data from unity is therefore a clear confirmation of the nuclear enhancement in the 2 GeV $\leq p_T \leq$ 6 GeV transverse momentum window. At low $p_T$ the ratio is smaller than unity, indicating absorption effects.

It is clear that the height of the Cronin peak depends on the extra $k_T$ broadening (quantitatively on the product $C \cdot h_{pA}(b)$), and Fig. 6 tells us that the location of the peak depends on the value of $\langle k_T^2 \rangle_{pp}$. Using our previously fixed parameters, NLO calculations at $Q = p_{T,jet}$ (solid lines) give the best fit to the experimental data (overlapping with LO curves at $Q = p_{T,jet}/2$, which curves not shown in Fig. 6, see Ref. [ 2]). In both cases the values of $\langle k_T^2 \rangle_{pp}$ are very much similar and $\langle k_T^2 \rangle_{pp} \approx 2$ GeV$^2$. This characteristic value of $\langle k_T^2 \rangle_{pp}$ is in good agreement with the experimental results of Ref. [ 29]. However, NLO calculations at $Q = p_{T,jet}/2$ (dashed lines) with much smaller $\langle k_T^2 \rangle_{pp}$ (see Fig. 3) give peaks shifted to unphysically low values of $p_T$. The sensitivity of the Cronin effect to the scale at the NLO level dictates our choice of scale in the present work.

### *3.3. Nucleus-nucleus collisions*

In nucleus-nucleus reactions, where both partons entering the hard collision originate in nucleons with additional semi-hard collisions, we do not need additional parameters, apply the Cronin enhanced width (7) for both initial partons. Thus,

$$E_\pi \frac{\mathrm{d}\sigma_\pi^{AB}}{\mathrm{d}^3p} = \int \mathrm{d}^2b\,\mathrm{d}^2r\; t_A(r)\; t_B(|\vec{b}-\vec{r}|)\; E_\pi \frac{\mathrm{d}\sigma_\pi^{pp}(\langle k_T^2\rangle_{pA}, \langle k_T^2\rangle_{pB})}{\mathrm{d}^3p}\ . \qquad (11)$$

For CERN energies we follow Fig. 4 and fix the values of $\langle k_T^2\rangle_{pp} = 1.6$ GeV$^2$ ($E_{beam} = 158$ AGeV) and 1.7 GeV$^2$ ($E_{beam} = 200$ AGeV) like in Ref. [ 2] for LO calculations. We keep $Q = p_{T,jet}$ and the Cronin parameters $\nu_m = 3$, $C = 0.35$ GeV$^2$.

In Fig. 7 the results of our calculation for $\pi^0$ transverse momentum spectra are compared to the WA80 [ 30] and WA98 [ 31] data on central $S+S$, $S+Au$, and $Pb+Pb$ collisions. Top panel shows the spectra, bottom panel displays the data/theory ratios. Dotted lines represent the results of the pQCD calculation with nuclear effects (shadowing and multiscattering) turned off, while solid lines correspond to the full calculation. (To test the effect of shadowing alone, we turned it off; the modification resulted in a $\leq 10\%$ downward shift in the spectra.) These calculations were performed down to $p_T = 1$ GeV; however, since pQCD is a theory of hard particle production, it is not expected to describe the data below $p_T \approx 2$ GeV.

In $S + S$ and $S + Au$ collisions the pQCD results reproduce the data at $p_T \geq 2.5 - 3$ GeV. In $Pb + Pb$ collisions we would expect a similar effect. However one can see a definite (upto 40%) overestimate in the calculation. The same result was obtained in the LO analysis (see Ref. [ 2]). The deviation of the data from the pQCD prediction indicates the appearance of a new collective effect in the $Pb + Pb$ collision. One candidate for this deviation is "jet quenching", the induced energy loss of high energy jets penetrating hot dense matter. This effect can be seen clearly at RHIC energy (see the data in Refs. [ 32, 33], and an explanation in Ref. [ 34]). Since jet quenching is strongly increasing with energy, its moderate appearance at CERN SPS in central $Pb + Pb$ collisions is acceptable.

## 4. Summary and conclusion

We presented a pQCD based parton model calculation in next-to-leading order powered by a jet-level $K$ factor. The intrinsic transverse momentum distribution of the partons inside nucleons was included into the model. The Gaussian width of this distribution in $pA$ and $AA$ collisions is controlled by two terms: the free $pp$ value $\langle k_T^2\rangle_{pp}$, fixed by several different experiments, and a nuclear part, which gives extra enhancement due to semihard collisions. (Note that at NLO level the factorization scale was chosen to be $Q = p_{T,jet}$.) While the nuclear part controls the height of the Cronin peak, the $\langle k_T^2\rangle_{pp}$ part determines its position.

We analyzed CERN SPS data and found that in $Pb + Pb$ collisions the experimental data are below the pQCD prediction by $30 - 40$ %. This is similar to what was seen in LO calculations[ 2]. With the present choice of scale and NLO

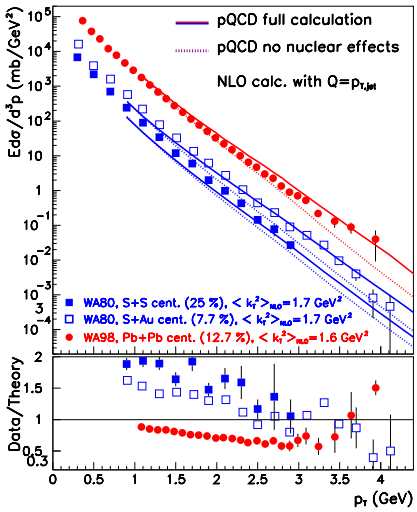


**Fig. 7.** Neutral pion production compared to data from SPS experiments WA80 and WA98 for central heavy ion collisions. Top panel shows the data and the calculated NLO invariant cross sections with the nuclear effects turned off (dotted lines) and for the full calculation (solid lines). Bottom panel displays the data/theory ratios for the full calculation.

approximation, the overestimation appears to be independent of the order of the pQCD calculation and indicates some collective nuclear effect. One candidate is the induced jet energy loss in hot dense matter ("jet-quenching"), which becomes significant in central $Pb + Pb$ collisions.

## Acknowledgments

This work was supported in part by U.S. DOE grant DE-FG02-86ER40251, NSF grant INT-0000211, FKFP220/2000 and Hungarian grants OTKA-T032796 and OTKA-T034842. Supercomputer time provided by BCPL in Bergen, Norway and the European Community − Access to Research Infrastructure action of the Improving Human Potential Programme is gratefully acknowledged.

## References


1. R.D. Field, *Applications of Perturbative QCD*, Addison-Wesley, 1995.
2. Y. Zhang, G. Fai, G. Papp, G.G. Barnaföldi, P. Levai Phys. Rev. C **65**, 034903 (2002).
3. G. Papp, P. Levai, and G. Fai, Phys. Rev. C **61**, 021902(R) (2000).
4. J.W. Cronin *et al.* (CP), Phys. Rev. D **11**, 3105 (1975).
5. D. Antreasyan *et al.* (CP), Phys. Rev. D **19**, 764 (1979).
6. G.G. Barnaföldi, G. Fai, P. Levai, G. Papp, Y. Zhang, J. Phys. G **27**, 1767 (2001).
7. S.D. Ellis, Z. Kunszt and D.E. Soper, Phys. Rev. Lett. **69**, 1496 (1992).
8. Z. Kunszt and D.E. Soper, Phys. Rev. D **46**, 192 (1992).
9. F. Aversa, M. Greco, P. Chiappetta and J.P. Guillet, Z. Phys. C **46**, 253 (1990); *ibid.* C **49**, 459 (1991).
10. R.K. Ellis and J.C. Sexton, Nucl. Phys. B **269** 445 (1986).
11. `http://zebu.uoregon.edu/~soper/soper.html`
12. M.A. Kimber, A.D. Martin, and M.G. Ryskin, Eur. Phys. J. C **12**, 655 (2000); Phys. Rev. D **63**, 114027 (2001).
13. B.A. Kniehl, G. Kramer, and B. Pötter, Nucl. Phys. B **597**, 337 (2001).
14. M. Glück, E. Reya, and A. Vogt, Z. Phys. C **53**, 127 (1992).
15. X.N. Wang, Phys. Rep. **280**, 287 (1997); Phys. Rev. Lett. **81**, 2655 (1998); Phys. Rev. C **58**, 2321 (1998).
16. C.Y. Wong and H. Wang, Phys. Rev. C **58**, 376 (1998).
17. C. Kourkoumelis *et al.* (R806), Z. Phys. C **5**, 95 (1980).
18. F.W. Büsser *et al.* (CCRS), Nucl. Phys. B **106**, 1 (1976).
19. D.E. Jaffe *et al.* (E605), Phys. Rev. D **40**, 2777 (1989).
20. P.B. Straub *et al.*, Phys. Rev. Lett. **68**, 452 (1992).
21. B. Alper *et al.* (ISR), Nucl. Phys. B **100**, 237 (1975).
22. G. Arnison *et al.* (UA1), Phys. Lett. B **118**, 167 (1983).
23. C. Albajar *et al.* (UA1), Nucl. Phys. B **335**, 261 (1990).
24. G. Bocquet *et al.* (UA1), Phys. Lett. B **366**, 434 (1996).
25. F. Abe *et al.* (CDF), Phys. Rev. Lett. **61**, 1819 (1988).
26. C.N. Brown, *et al.*, Phys. Rev. C **54**, 3195 (1996).
27. X.N. Wang and M. Gyulassy, Phys. Rev. D **44**, 3501 (1991).
28. K.J. Eskola, V.J. Kolhinen, and C.A. Salgado, Eur. Phys. J. C **9**, 61 (1999).
29. M.D. Corcoran *et al.* (E609), Phys. Lett. B **259**, 209 (1991).
30. R. Albrecht *et al.* (WA80), Phys. Lett. B **361**, 14 (1995).
31. M.M. Aggarwal *et al.* (WA98), Phys. Rev. Lett. **85**, 3595 (2000); Eur. Phys. J C **23**, 225 (2002); nucl-ex/0006007.
32. W.A. Zajc for the PHENIX Coll., Nucl. Phys. A **698**, 39c (2002); G. David for the PHENIX Coll., Nucl. Phys. A **698**, 227c (2002).
33. J.W. Harris for the STAR Coll., Nucl. Phys. A **698**, 64c (2002).
34. P. Levai, G. Papp, G. Fai, M. Gyulassy, G.G. Barnaföldi, I. Vitev, Y. Zhang, Nucl. Phys. A **698**, 631c (2002).